ELSEVIER

NeuroImage

www.elsevier.com/locate/ynimg
NeuroImage 25 (2005) 1325–1335

Technical Note

A new SPM toolbox for combining probabilistic cytoarchitectonic maps and functional imaging data

Simon B. Eickhoff,[a,b] Klaas E. Stephan,[c] Hartmut Mohlberg,[a] Christian Grefkes,[a,b,d] Gereon R. Fink,[a,d,e] Katrin Amunts,[a,e,f] and Karl Zilles[a,b,e,*]

[a]*Institut für Medizin, Forschungszentrum Jülich, Jülich, Germany*
[b]*C. and O. Vogt Institut für Hirnforschung, Düsseldorf, Germany*
[c]*Wellcome Department of Imaging Neuroscience, University College London, UK*
[d]*Neurologische Klinik, Universitätsklinikum Aachen, Germany*
[e]*Brain Imaging Center West (BICW), Jülich, Germany*
[f]*Klinik für Psychiatrie und Psychotherapie, Universitätsklinikum Aachen, Germany*

Received 10 August 2004; revised 10 December 2004; accepted 14 December 2004
Available online 3 March 2005

Correlating the activation foci identified in functional imaging studies of the human brain with structural (e.g., cytoarchitectonic) information on the activated areas is a major methodological challenge for neuroscience research. We here present a new approach to make use of three-dimensional probabilistic cytoarchitectonic maps, as obtained from the analysis of human post-mortem brains, for correlating microscopical, anatomical and functional imaging data of the cerebral cortex. We introduce a new, MATLAB based toolbox for the SPM2 software package which enables the integration of probabilistic cytoarchitectonic maps and results of functional imaging studies. The toolbox includes the functionality for the construction of summary maps combining probability of several cortical areas by finding the most probable assignment of each voxel to one of these areas. Its main feature is to provide several measures defining the degree of correspondence between architectonic areas and functional foci. The software, together with the presently available probability maps, is available as open source software to the neuroimaging community. This new toolbox provides an easy-to-use tool for the integrated analysis of functional and anatomical data in a common reference space.

Keywords: Functional magnetic resonance imaging; Structure; Mapping; Atlas; PET

Introduction

Functional magnetic resonance imaging (fMRI) and positron emission tomography (PET) provide information about the functional organization of the human cerebral cortex with a spatial resolution in the range of a few millimeters. Several concepts can be applied for the anatomical interpretation of functional activations, e.g., stereotaxic coordinates or macroanatomical landmarks. These concepts, however, do not appropriately take into account the microscopical architectonic organization of the human brain (Amunts and Zilles, 2001; Zilles et al., 2002). In turn, there is plenty of evidence from studies of non-human primates that the microstructure and connectional architecture of the cortex are the main determinants of the regional segregation of its functions (e.g., Luppino et al., 1991; Matelli et al., 1991). Consequently, there is a general consensus that cortical areas, defined by their microstructure and/or connectivity, can be regarded as functional modules of the cortex (for reviews, see Felleman and Van Essen, 1991; Passingham et al., 2002). Therefore, the anatomical interpretation of functional imaging results with respect to microstructurally defined areas is the most appropriate topographical reference for regionally specific activations observed in functional imaging studies.

One of the most widely used anatomical references is the brain atlas of Talairach and Tournoux (1988). This atlas was seminal for the development of functional neuroimaging by introducing a spatial reference system for the human brain, which is independent of skull landmarks: the reference brain is an individual post-mortem brain, which is aligned according to a plane defined by the anterior and posterior commissures (AC–PC plane). Stereotaxic locations are then described in coordinates relative to the origin (coordinates 0,0,0) defined by the intersection of the AC with the interhemispheric plane.

The use of "Talairach labels" for the cytoarchitectonic allocation of functional activations is, however, problematic for several reasons. The atlas does not provide information with respect to the inter-individual variability of the cytoarchitectonic areas or the relative probabilities for different areas at a given position. This causes the impression that a stereotaxic location necessarily belongs to a specific cortical area, although recent and previous

* Corresponding author. Institut für Medizin, Forschungszentrum Jülich GmbH, D-52425 Jülich, Germany. Fax: +49 2461 61 2990.
E-mail address: K.Zilles@fz-juelich.de (K. Zilles).
Available online on ScienceDirect (www.sciencedirect.com).

1053-8119/$ - see front matter © 2004 Elsevier Inc. All rights reserved.
doi:10.1016/j.neuroimage.2004.12.034

cytoarchitectonic studies demonstrate considerable inter-individual differences in size and location of cortical areas (Amunts et al., 2000; Geyer et al., 1999; von Economo and Koskinas, 1925).

More importantly, the cytoarchitectonic labels shown in the Talairach atlas are not based on a microstructural analysis. Rather, the authors inferred, based on sulcal landmarks and gross morphology, where the areas depicted on Brodmann's (1909) map could be located in this subject. Many studies have demonstrated, however, that the borders of microstructural areas do not always show a precise and reliable relationship to macroanatomical landmarks (Amunts et al., 1999; Geyer et al., 1999; Grefkes et al., 2001; Zilles et al., 2002). For example, BA 44 usually occupies the opercular part of the inferior frontal gyrus, whereas BA 45 is found on the triangular part. However, BA 44 can also encroach on the triangular part and BA 45 may also reach aspects of the opercular part, respectively. Similarly, BA 44 may border BA 6 in either the anterior or the posterior bank of the precentral sulcus (Amunts et al., 1999, 2004). Furthermore, the correspondence between macroanatomical features and microstructural areas is quite variable across the cortex. Particularly, it is frequently not possible to correlate the borders of cytoarchitectonic areas with macroscopical landmarks, whereas centers of a cytoarchitectonic area may be well identified by macroscopical features (e.g., the borders of the primary visual cortex V1, which is always found in the calcarine sulcus, vary considerably regarding sulcal features). Although there is a reliable relationship for some areas like the primary cortical area 3b, the correspondence is much worse in other regions of the brain, in particular in parietal or frontal association areas.

As an alternative to the post-mortem reference brain of the Talairach and Tournoux atlas, fMRI or PET data are often normalized to the templates provided by the Montreal Neurological Institute (MNI). The most widely used MNI templates are a single-subject template and a group template created from 152 individual brains, both aligned to the Talairach-like MNI305 reference space (Collins et al., 1994; Evans et al., 1992; Holmes et al., 1998). Although these templates are roughly based on the Talairach space, they do not match the Talairach brain in size and shape (Brett et al., 2002).

In contrast to classical cytoarchitectonic maps (e.g., Brodmann, 1909), probabilistic cytoarchitectonic maps provide stereotaxic information on the location and variability of cortical areas in the MNI reference space (Amunts and Zilles, 2001; Mohlberg et al., 2003; Zilles et al., 2002). They are based on the observer-independent analysis of the cytoarchitecture in a sample of ten human post-mortem brains. Such maps have been published for various brain regions, including the motor, somatosensory, visual, auditory, and language related areas (Table 1).

Table 1
List of probabilistic cytoarchitectonic maps published in journal articles or monographs

Primary auditory cortex (Te 1.0, 1.1, 1.2)	Morosan et al., 2001; Rademacher et al., 2001
Broca's region (BA 44, 45)	Amunts et al., 1999, 2004
Primary motor cortex (areas 4a, 4p)	Geyer et al., 1996
Premotor cortex (BA 6)	Geyer, 2003
Primary somatosensory cortex (BA 3a, 3b, 1)	Geyer et al., 1999, 2000b
Somatosensory cortex (BA 2)	Grefkes et al., 2001
Visual cortex (BA 17, 18)	Amunts et al., 2000

Further cortical and subcortical regions are currently under investigation.

Several studies have used these maps for the anatomical interpretation of functional imaging experiments analyzing, e.g., motor somatosensory and language processing (e.g., Amunts et al., 2004; Binkofski et al., 2002; Bodegard et al., 2001; Naito et al., 1999). The results of these studies show that the combination of functional imaging with cytoarchitectonic data can greatly enhance the structural information behind functional imaging experiments. However, the methods for combining cytoarchitectonic maps and functional imaging data had to be set up individually for each study. One reason for this time-consuming task is that the probabilistic cytoarchitectonic maps have not yet been integrated into a standard neuroimaging software package.

One of the most popular packages for the analysis of functional imaging data is SPM2 (The Wellcome Dept. of Imaging Neuroscience, London; www.fil.ion.ucl.ac.uk/spm). We here introduce a new SPM toolbox enabling the comparison of cytoarchitecture and function in this software environment to provide a routine, standardized application of probabilistic cytoarchitectonic maps as an anatomical reference for functional activations. The features of this toolbox include:

i) The display and statistical description of the probabilistic maps for each cytoarchitectonic area in stereotaxic space.
ii) The combination of the individual maps into a summary map to define non-overlapping volumes of interest for each area.
iii) The description of the anatomical location of functional activation clusters and local maxima.
iv) The functional characterization of anatomical areas by evaluating their response to different experimental conditions.

Overview of the method

The "SPM Anatomy toolbox" was developed for the integration of cytoarchitectonic probabilistic maps of the human cerebral cortex into the SPM software package. It consists of a set of scripts coded in the platform-independent MATLAB programming language (The MathWorks Inc., Natick, MA). Only the core version of MATLAB (version 5.5 or above) is required, no additional extensions are necessary. In combination with the freely available probability maps, the SPM Anatomy toolbox handles all of the steps necessary for an integrated analysis of structural and functional data, e.g., the visualization and statistical description of probabilistic maps, the generation of summary maps combining the information of the different probabilistic maps and finally the anatomical interpretation of functional imaging results using different measures of correspondence as described below. Since the functional analysis can be performed entirely within SPM, no specific requirements on the experimental setup or statistical analysis of the functional data are enforced. Rather, functional imaging data can be analyzed using all options offered by SPM2 including available toolboxes and extensions. The SPM Anatomy toolbox is also compatible with data processed in SPM99. Statistical maps, which have been calculated using alternative functional image analysis programs, such as AFNI (http://afni.nimh.nih.gov/afni/), FSL (http://www.fmrib.ox.ac.uk/fsl) or FMRISTAT (http://www.math.mcgill.ca/keith/fmristat/) can also be analyzed using the SPM Anatomy toolbox. The statistical maps resulting from the analyses in these programs which were saved in analyze or MINC volumes can be loaded and thresholded by the

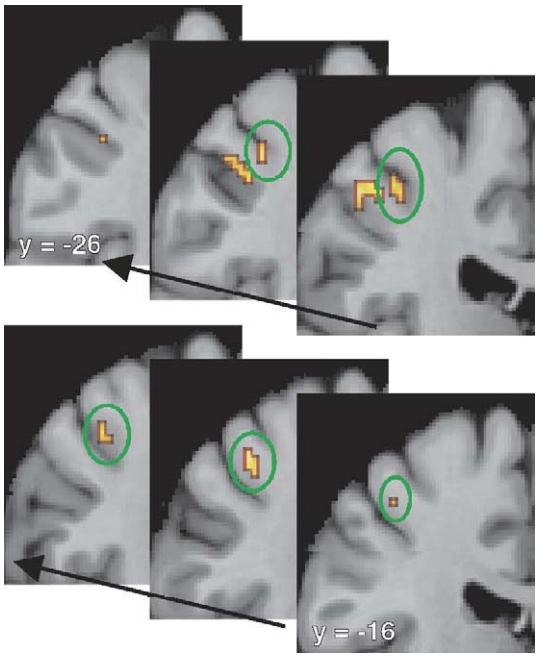

Fig. 1. Neural activations associated with tactile processing of 3D objects (Grefkes et al., 2002). Projection of the significant activations in the contrast between the purely tactile (TT) and the purely visual (VV) conditions (random effects group analysis, $P < 0.05$ corrected at the voxel level) onto coronal sections (left hemisphere) of the reference brain. All coordinates refer to anatomical MNI space. Two separate clusters of activation can be identified in the region of interest, one on the post- and one on the precentral gyrus. The latter one (marked by the green circle) is discussed further in the text as an illustration of the use of probabilistic cytoarchitectonic maps for the anatomical interpretation of fMRI data.

SPM Anatomy toolbox to correlate the statistically significant activations with the cytoarchitectonic maps.

Example fMRI data

The functionality of the SPM Anatomy toolbox is illustrated using an fMRI experiment in which 12 subjects encoded and subsequently recognized abstract three-dimensional objects (Grefkes et al., 2002). During the experiment, the objects were either presented visually on a video screen or tactually explored with the right hand. The experimental design consisted of four conditions: tactile encoding and recognition (TT), tactile encoding and visual recognition (TV), visual encoding and tactile recognition (VT) and finally visual encoding and recognition (VV). The analysis used a random effects model (significance threshold of $P < 0.05$, corrected for multiple comparisons). The original analysis focused on the aspect of cross-modal object recognition (e.g., visual recognition of a tactually encoded object), which activated anterior intraparietal cortex (Grefkes et al., 2002). We now demonstrate the cytoarchitectonic correlates of the activation maximum on the precentral gyrus during unimodal tactile information processing (TT > VV) at $x = -38$,$y = -22$, $z = +63$, reflecting the larger requirements on motor and somatosensory processing during tactile (as compared to visual) processing (Fig. 1).

Probabilistic cytoarchitectonic maps in stereotaxic space

The observer-independent definition of cytoarchitectonic areas and the generation of probabilistic maps have been described in detail in the publications, which report the results of cytoarchitectonic mapping studies (Table 1). These methods are also summarized in Flowchart 1.

The probabilistic maps are located in the space of the T1 weighted MNI single subject template (Collins et al., 1994; Evans et al., 1992; Holmes et al., 1998). The origin of the MNI space is located 4 mm more caudally (y axis) and 5 mm more dorsally (z axis) than the intersection between the AC and the interhemispheric fissure in this specific brain. To keep the AC as the anatomical reference of the coordinate system, the origin of the probabilistic maps was corrected for this displacement. The correction results in the so called "anatomical MNI space," which differs from the original MNI space by an affine translation along the y and z axes of 4 and 5 mm, respectively. When using these maps for structure–function analysis, the user is prompted, whether the functional data have been normalized to the templates in standard MNI space as provided by SPM2 or the corresponding templates in anatomical MNI space as used by the SPM Anatomy toolbox. If the functional data have been normalized into the standard MNI space, the SPM Anatomy toolbox automatically applies the linear correction to the anatomical MNI space. All locations are then reported both in standard and anatomical MNI coordinates.

It should be noted that the individual post-mortem brains were normalized to this template by using a high-dimensional elastic multigrid warping algorithm, which provides precise registrations, in particular with respect to the cortical gray matter at a resolution

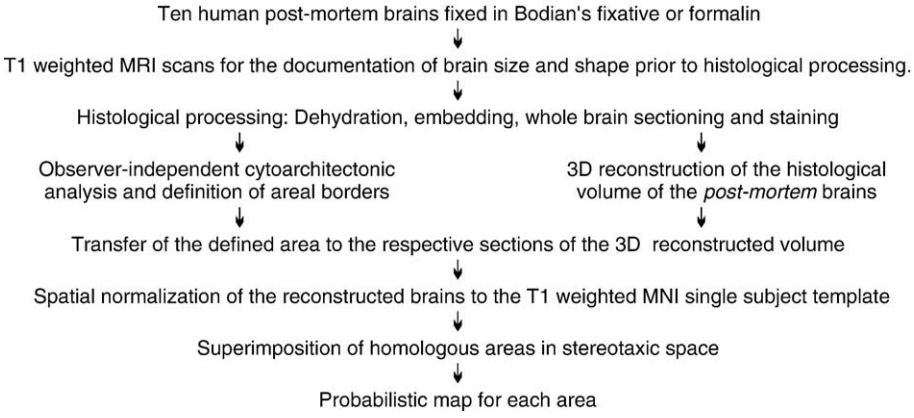

Flowchart 1. Overview on the processing steps necessary for the generation of probabilistics cytoarchitectonic maps.

of 1 × 1 × 1 mm^3 (Amunts et al., 2004; Mohlberg et al., 2003). Given the large number of available image registration methods, which all have their advantages and drawbacks, and the methodological difficulties intrinsic to any comparison between them, no prerequisite is imposed by the SPM Anatomy toolbox on the method used for the spatial normalization of the functional data. Rather, the users should always take into consideration that discrepancies between functional and anatomical localizations might result from the use of different algorithms and thus check the plausibility of all results by comparison with the mean anatomical image of the examined group of subjects after normalization.

The probabilistic maps describe, for each voxel of the reference space, the frequency with which a cytoarchitectonic area was observed at this specific position in the sample of ten post-mortem brains (Fig. 2). Evidently, the respective probabilities can only change in increments of 10%. The program calculates the center of gravity of the cytoarchitectonic area for each hemisphere and shows the volume associated with a cortical area at different probabilities. The maximum stereotaxic coordinates (bounding box) for the cytoarchitectonic area are given based on two calculations: (i) including all voxels where the respective area is found and (ii) including only those voxels where the probability is at least 50% (Fig. 2). Evidently, high probabilities are only found for a small number of voxels, whereas small probabilities (e.g., two out of ten, 20%) are found for a larger number of voxels. This relationship reflects the high variability in size and location of corresponding cortical areas between different subjects. As a consequence of the increasing volumes, the probabilistic maps for different areas overlap at lower probabilities (Fig. 3). Due to this overlap, some voxels of the reference space can be associated to more than one cortical area.

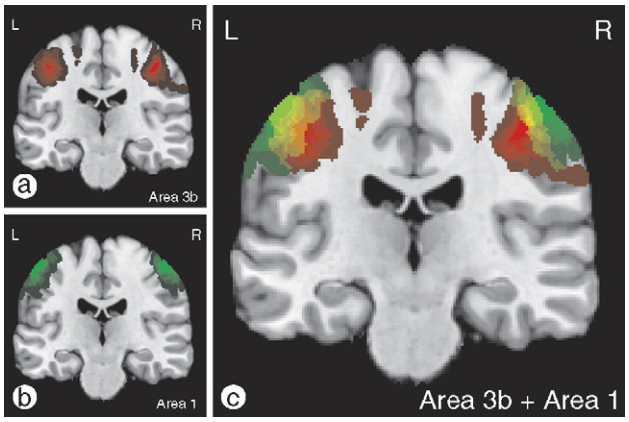

Fig. 3. Two coronal sections through the T1 weighted MNI single-subject template at $y = -25$ in anatomical MNI space (i.e. $y = -21$ in the original MNI space), showing the probabilistic maps of BA 3b (a) and BA 1 (b). Note the considerable overlap in the probabilistic maps of these two (neighboring) cortical areas, illustrated in panel (c), which shows both probabilistic maps superimposed on each other.

Maximum probability map

For the comparison with functional imaging data, a summary map was computed by the SPM Anatomy toolbox from the 14 probabilistic maps listed in Table 1. It defines the most likely cytoarchitectonic area at each voxel ("maximum probability map,"

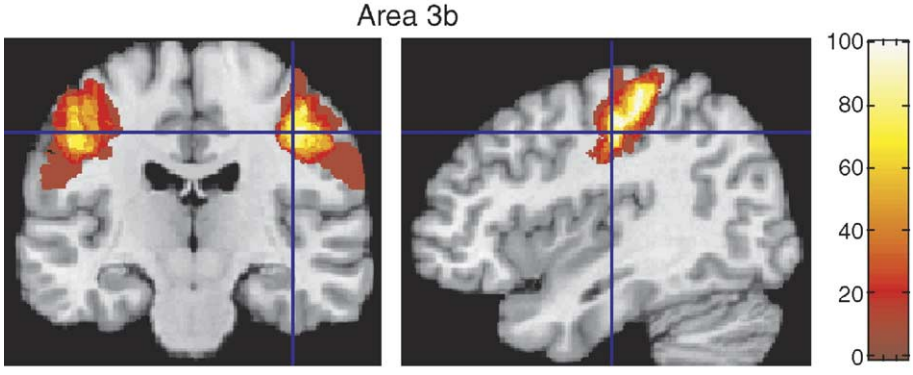

Crosshair position: x=41, y=-22, z=48
Probability for Area 3b : 90%

Prob.	left (mm^3)	right (mm^3)
10 %	20005	14715
20 %	9717	7591
30 %	6037	5196
40 %	3579	3729
50 %	2207	2732
60 %	1256	1868
70 %	620	1156
80 %	169	599
90 %	21	310
100 %	1	86

	left (x / y / z)		
Center	-37	-28	54
Minimum	0	-62	8
Maximum	-68	11	87
50% min.	-10	-48	26
50% max.	-61	-6	76

	right (x / y / z)		
Center	37	-28	55
Minimum	1	-57	15
Maximum	69	1	88
50% min.	5	-51	20
50% max.	66	-3	80

Fig. 2. Orthogonal sections and statistics for the probabilistic map of BA 3b (Geyer et al., 2000b). All coordinates are in anatomical MNI space (i.e. origin defined by the AC).

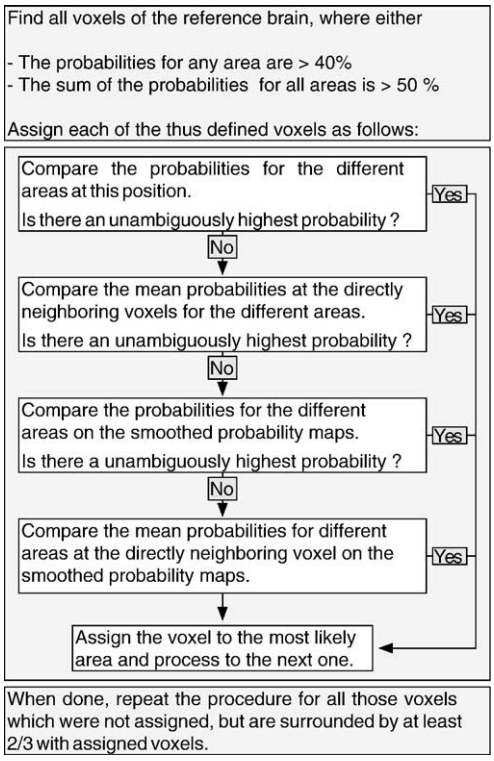

Flowchart 2. Algorithm used for the generation of the maximum probability map.

MPM) as outlined in Flowchart 2 and hereby allows the definition of non-overlapping volumes of interest for each area. The visualization by the MPM (Figs. 3 and 4) is thus similar to conventional brain atlases, e.g., that of Talairach and Tournoux. In contrast to this map, however, the MPM is based on a sample of 10 post-mortem brains, not on a single hemisphere.

For each voxel, the numbers of overlapping representations, which were observed for the different cytoarchitectonic area, are compared. The voxel is then assigned to that area, which shows the highest probability (i.e. the greatest overlap among the ten examined post-mortem brains) at this particular position. There are several voxels, in which different areas may show equally high probabilities. A voxel, which, according to this procedure, has more than one most likely areas, is assigned to that area, which shows the higher average probability in the 3 × 3 × 3 neighborhood (i.e. in a 3 × 3 × 3 voxel cube centered at the location in question). In rare cases where still no definitive allocation to a single area is possible, the procedure is repeated on probability maps smoothed using an isotropic Gaussian kernel. As a reasonable rule, the FWHM of this kernel should be close to the smoothing filter applied to the functional data.

It should be noted that the 14 cytoarchitectonically delineated areas do not cover the entire cortex (Fig. 4). Therefore, the approach described above could overestimate the spatial extent of a delineated area at its borders towards unmapped cortex. For example, consider the transitional region between area 2 and the cortex posterior to it (Fig. 4). While many voxels in this region show only low probabilities for belonging to area 2, their probabilities for belonging to area 5 (which is not included in the cytoarchitectonic atlas yet) are unknown. Therefore, a decision based on maximum known probabilities alone could falsely assign these voxels to area 2. To correct for this putative source of error, an absolute probability threshold was determined by examining the probabilities at the borders between defined cytoarchitectonic areas, i.e. in all those regions where the probabilistic maps overlap between two adjacent areas. The median fraction used to assign those voxels to one of these areas was 0.428. Thus, the majority of voxels assigned at these border zones had a probability of 4/10 or more. Assuming similar probability distributions at the borders towards unmapped regions, the threshold for including a voxel into the MPM was set to 4/10 (i.e. ≥40% probability). The voxels, in which the most likely area shows a lower probability, are not assigned to any area. However, to ensure the continuity of the resulting summary map, voxels are also included (i) if the cumulative probability of this voxel across all areas is at least 60% (that is, cytoarchitectonically mapped areas were found at this position in more than half of the examined brains) or (ii) if more than 2/3 of the surrounding voxels are assigned to cortical areas. The first of these two criteria (cumulative probability) accounts for 6.2% and the latter (surrounding voxels) for 2.7% of the total volume of the MPM.

The resulting maximum probability map (MPM) provides volumes of interest for each area, yielding a continuous, non-overlapping parcellation of the cerebral cortex (Fig. 4). In total,

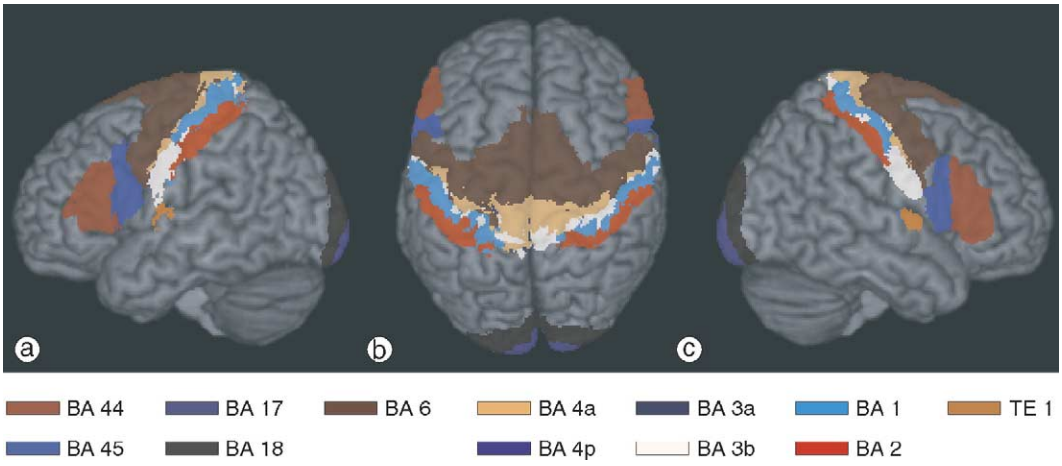

Fig. 4. Surface rendering of the T1 weighted MNI single-subject template and the maximum probability map (MPM) of all probabilistic maps of cortical areas published to date. Only the surface extent of the different areas is shown. (a) Lateral view on the left hemisphere, (b) dorsal view, (c) lateral view on the right hemisphere.

263.390 voxels (volume: 1 mm^3 each) are assigned to the 14 cytoarchitectonic areas listed in Table 1. 91.6% (241.230) of these voxels are assigned in the first step based on the relative probabilities. 8.2% voxels (21.621) are assigned following comparison of the neighboring voxels, the remaining 0.2% voxels (539) by the use of the smoothed probability maps.

The correspondence between the anatomy of the single subject template of the MNI and the MPM is illustrated in Fig. 5. The region around the central sulcus shows a relatively stable relationship between its macroanatomy (i.e. gyri and sulci) and the location of the cortical areas: for example, BA 3a is known to be located in the fundus of the central sulcus whereas BA 1 is located on the crown of the postcentral gyrus (Geyer et al., 1999). This relationship is well preserved in the MPM.

Anatomical localization of functional activations

The analysis of the correlation between structure and function is the main part of the SPM Anatomy toolbox. After computation of the contrasts and thresholding of the SPM{T} or SPM{F} maps as part of the functional analysis, each significant activation is projected onto orthogonal sections of the MPM (Fig. 6). This step enables the visual inspection of the location of the activation foci with respect to architectonically defined cortical areas. The cytoarchitectonic allocations of each significant cluster of activation can then be described in different quantitative terms (Flowchart 3).

(1) Cluster labeling

To assess the position of a functional activation cluster relative to cytoarchitectonic areas, the volume of this cluster is compared to the MPM using a cluster labeling method (Binkofski et al., 2002; Naito et al., 1999; Tzourio-Mazoyer et al., 2002). For this analysis, the overlap of the examined functional cluster with the different cytoarchitectonic areas is computed. The relative overlap with each area is then calculated as the percentage of the overlapping voxels relative to the total number of activated voxels in this cluster. For example, the major part (~80%) of the activation on the precentral gyrus (Fig. 1) is located in BA 4 (areas 4a + 4p, Geyer et al., 1996) as shown by a comparison with the MPM (Fig. 6). This result is in good accordance with the macroscopical localization of this activation on the posterior wall of the precentral gyrus, where area 4 is located (Geyer et al., 1996, 2000a). Smaller parts of the activation are encroaching upon BA 6 (12.5%), i.e. in the neighboring agranular premotor cortex (Geyer, 2003), and in primary somatosensory area 3b (7.5%, Geyer et al., 1999). Interestingly, the two subdivisions of the primary motor cortex (areas 4a and 4p), are activated to a similar degree: 42.5% of the cluster is located in area 4p and 37.5% in area 4a.

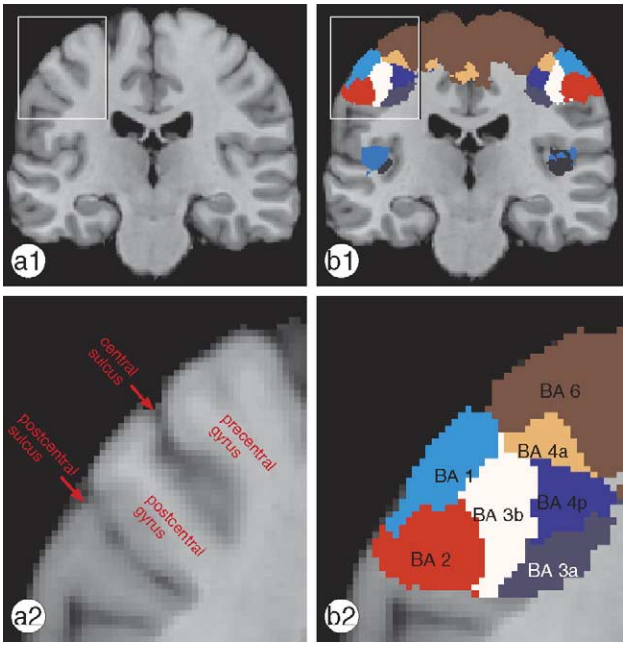

Fig. 5. (a) Coronal sections through the T1 weighted MNI single-subject template at $y = -21$ (same plane as in Fig. 2) Coordinates in anatomical MNI space. (a1) Whole section (a2) view zoomed on the region around the central sulcus as indicated by the white box in panel (a1). (b) Projection of the (color coded) maximum probability map (MPM) onto this section and its detailed view. The cytoarchitectonic assignments of the MPM are shown in panel (b2).

(2) Relative extent of activation

The overlap can also be described relative to the size of the cytoarchitectonic areas: here, the number of "activated" voxels is expressed as a percentage of the total number of voxels assigned to this area (Bodegard et al., 2001, Young et al., 2004). This allows inferring whether a cortical area is widely activated in a given contrast or whether the activation is focused on a smaller region within this area. The latter would be expected, e.g., in somatotopically or retinotopically organized areas. This is also observed in our example data set, where the task involved movement of the hand only. The significantly activated cluster consequently does not extend over more than 1.4% of any of the four areas (4a, 4p, 3b and BA 6, Fig. 6). The calculated extent of activation for the displayed contrast is thus very small, even considering the quite rigid statistical threshold ($P < 0.05$ corrected).

It should be noted that the information on the extent of an activation and the cluster labeling described above reflect complementary aspects of data analysis: While cluster labeling characterizes the correspondence between structure and function from the perspective of the functional activation, analyzing the relative extent of an activation takes the perspective of the cytoarchitectonic area. By necessity, the results of both methods depend upon the statistical threshold used in the analysis of the functional imaging data.

(3) Local maxima labeling

When the statistical analysis reveals large clusters of activation, which may cover several cortical areas, it can be very helpful to examine the (probabilistic) anatomical location of the different local maxima within these clusters (Amunts et al., 2004). The anatomical location of a given voxel (e.g., a maximum) can be described by answering the following questions: is this voxel assigned to a cytoarchitectonic area in the MPM? What are the probabilities of cytoarchitectonic areas at that position? In this context, it has to be considered that the spatial resolution of the probabilistic maps (1 mm voxel size) is considerably higher than the resolution of the functional images, which is usually 2–4 mm voxel size after resampling during spatial normalization. The probability for the directly corresponding voxel may therefore over- or underestimate the anatomical probabilities due to interpolation. To increase the reliability of the anatomical allocation, the probability at the directly corresponding voxel as

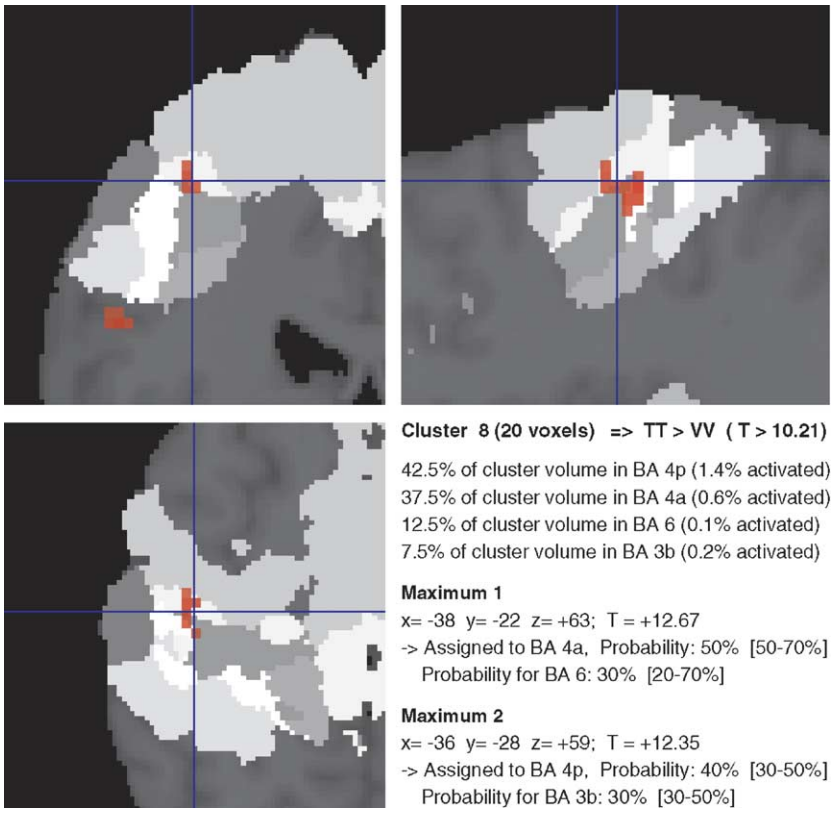

Fig. 6. Screenshot from the SPM Anatomy toolbox showing the anatomical interpretation of the previously mentioned functional cluster (Fig. 1): the functional activation is overlaid on the gray level coded MPM on orthogonal sections to allow a visual inspection (upper left: coronal view, upper right: saggital view, lower left: axial view). The display is zoomed in on the location of the functional activation. The field of view approximately matches that in Fig. 5b2. The quantitative analysis on the correspondence between structure and function is displayed next to the orthogonal sections. All graphical user interface elements have been remove from the screenshot for the sake of clarity.

well as the probability range for the surrounding voxels are calculated by the SPM Anatomy toolbox. This procedure also takes into account that the *effective* resolution of the anatomical maps might be somewhat reduced due to the inevitable imperfections in the spatial normalization.

For example, the highest maximum (T value = +12.67) of the motor activation shown in Figs. 1 and 6 is located at $x = -38$, $y = -22$, $z = +63$ (all coordinates are anatomical MNI coordinates). Its location is assigned to area 4a, as the probability for this area is 50% (50–70% for the surrounding voxels), whereas the probability

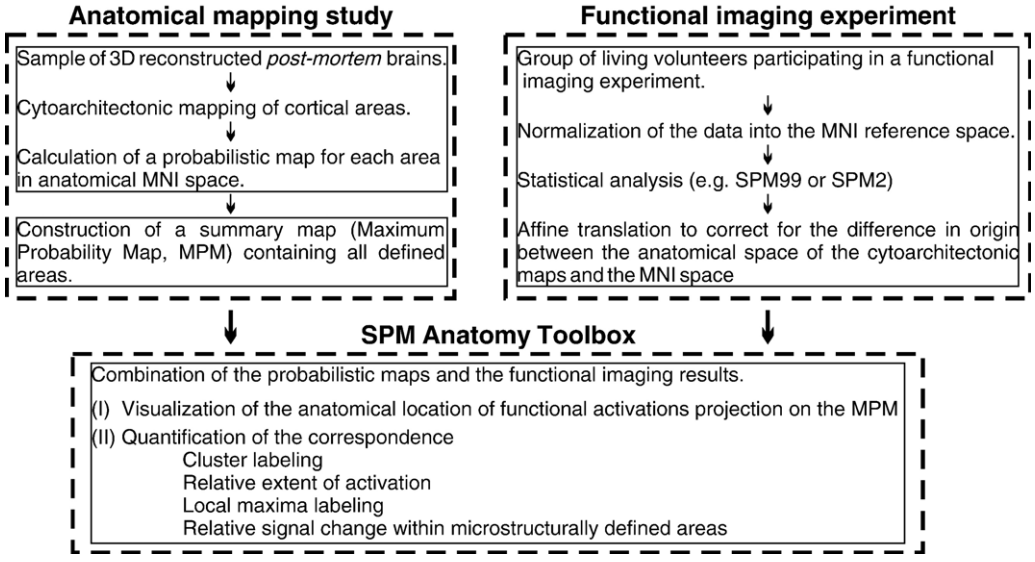

Flowchart 3. Combining anatomical and functional data: overview on the methodology.

for BA 6 is only 30% (20–70%). A second peak (T value =+12.35) is found at $x = -36$, $y = -28$, $z = +59$ and assigned to area 4p. At that position, the probability of finding area 4p is 40% (30–50% for the surrounding voxel), whereas the probability of finding BA 3b is 30% (30–50%). Thus, the functional cluster of activation may actually reflect two distinct activations (within areas 4a and 4p, respectively), which are merged into a single cluster of increased activation because of the limited spatial resolution of functional (group) analysis.

(4) Relative signal change within microstructurally defined areas

The relative signal change (e.g., rCBF in PET, BOLD in fMRI) within a cytoarchitectonic area evoked by the different experimental conditions can be used to examine the involvement of that particular area in a specific tasks. This can be of interest, for example, in random effects analyses where the inference pertains to inter-subject variance. Therefore, small signal changes can lead to highly significant activations if they are found consistently across subjects (Grefkes et al., 2002; Manjaly et al., 2003). To obtain the percent signal change for each condition, we computed the ratio between the condition-specific signal change (by multiplying its parameter estimate with the height of the corresponding regressor from the filtered design matrix) and the mean signal during the session (represented by the product of the parameter estimate for the constant term in the model and the height of its regressor in the filtered design matrix). This relative signal change can be calculated (i) for individual voxels e.g., at the position of the local maximum, (ii) as averages across all voxels assigned to a specific cytoarchitectonic area in the maximum probability map or (iii) for the "center" of an area including voxels in the upper 10 percentile of its probability distribution. This kind of analysis enables the analysis of differential activations of these areas independent of contrast definitions and statistical thresholds.

The condition-wise percent BOLD signal change for both subregions of the left primary motor cortex in our example data set is shown in Fig. 7. Some of the response characteristics are very similar in areas 4a and 4p, although the BOLD response is generally weaker in area 4a, i.e. the anterior part of the primary motor cortex. Both areas show a decrease in the BOLD signal in the purely visual condition (VV: visual encoding and recognition) and a strong increase in the BOLD signal during the purely tactile condition (TT: tactile encoding and recognition). Notable differences are found in the cross-modal conditions: In particular, there is no significant ($P > 0.001$) change in the BOLD signal within area 4a associated with the condition TV, where subjects had to tactually encode objects and subsequently recognize them visually. In contrast, there is a significant ($P < 0.001$) BOLD signal increase for that condition in area 4p. Thus, only the posterior but not the anterior part of BA 4 seems to be activated in haptic exploration and encoding of complex object. This differential activation of areas 4a and 4p may be related to the higher attentional modulation shown for area 4p as compared to 4a (Binkofski et al., 2002). This example demonstrates the possibility of analyzing functional data based on a-priori anatomical knowledge and highlights the potential that such an analysis approach may lead to new perspectives on a brain region's specific function.

Discussion

Functional neuroimaging has reawakened the interest in the microstructural organization of the human brain, given the demand for an anatomical reference when interpreting functional imaging results. In parallel to this growing need, new techniques have emerged in the field of anatomical brain mapping, which allow for an observer-independent definition of cortical borders and the generation of three-dimensional probabilistic maps (Amunts and Zilles, 2001; Roland and Zilles, 1994; Schleicher et al., 1998; Zilles et al., 2002). These maps combine the details of (cyto-) architectonic examination with a representation of the results in a three-dimensional reference space.

We here present a new software package enabling the use of these maps within the SPM environment to incorporate the

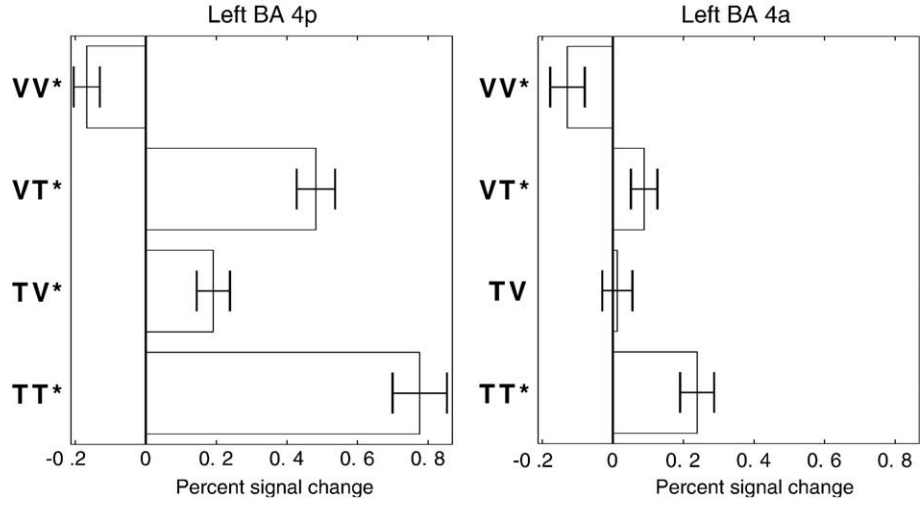

Fig. 7. Screenshot from the SPM Anatomy toolbox showing the percent signal change within BA 4a and BA 4p (voxels in the upper 10 percentile of the probability distribution). Each area is represented by the 10% of the assigned voxel, which showed the highest probability for the respective area. The corresponding percent signal changes of the BOLD signal evoked by the different conditions within the two areas are shown as bar charts (mean and standard error for the group of 12 subjects): VV, visual object encoding and recognition; VT, visual encoding and tactile recognition; TV, tactile encoding and visual recognition; TT, tactile object encoding and recognition. Asterisks denote significant ($P < 0.001$) changes of the BOLD signal for that condition compared to baseline. Note that condition TV (tactile encoding and visual recognition) did evoke a significant change in the BOLD signal in BA 4a, but not in 4p.

knowledge gained by cytoarchitectonic mapping studies of the human cerebral cortex into the interpretation of functional imaging data and vice versa. As illustrated by the example data set presented above, the SPM Anatomy toolbox provides the user with a detailed, quantitative description of the anatomical location of functional imaging clusters based on different aspects of the correspondence between structure and function.

Although there are several tools available for the anatomical labeling of functional imaging results, this is the first software package which provides probabilistic anatomical labels based on observer-independent microstructural analysis of the human cerebral cortex in a sample of post-mortem brains. Existing programs, which provide anatomical labels for functional data relied on macroanatomically defined brain regions (Crespo-Facorro et al., 1999; Kim et al., 2000; Tzourio-Mazoyer et al., 2002) or landmark-based comparisons with the Talairach atlas (Lancaster et al., 1997, 2000; Maldjian et al., 2003). Using probabilistic cytoarchitectonic maps instead of "Talairach labels" overcomes many of the methodological disadvantages and possible sources of error associated with the use of the Talairach and Tournoux atlas. These new maps are available in the MNI reference space and thus directly comparable to functional imaging data, they provide probabilities for finding different cytoarchitectonic areas at a specified position and, in contrast to the Talairach and Tournoux atlas, they are based on genuine cytoarchitectonic analysis in a sample of post-mortem brains.

It is evident from Fig. 4 that the MPM computed from the yet available cytoarchitectonic maps does not cover the entire cortical surface. Rather, the cytoarchitectonic mapping has been started with early sensory and motor areas since these areas show the most distinct architecture. For some cortical regions, these areas have provided "anchor points" for the examination of the surrounding higher order association cortex. Of course, the database of cytoarchitectonic maps is open and strongly growing as new areas are constantly being mapped. Once new probabilistic maps are available, it will be included into the SPM Anatomy toolbox. Until a complete atlas of cytoarchitectonic maps is available, macroanatomical labels (e.g., "right middle frontal gyrus," Tzourio-Mazoyer et al., 2002) are provided by this software for functional activations which are located outside the available probabilistic cytoarchitectonic maps.

Importantly, the probabilistic approach for the anatomical allocation of functional activations is much closer to the idea of random effects analysis, which now has become the standard in functional neuroimaging. In random effects analysis, the observed effect is compared to the variability between subjects to make inferences about the general population. The results, which are then compared to an anatomical atlas, are thus the effects observed in a group of subjects. Consequently, they can only be labeled adequately by comparison with anatomical data from a *group* of microstructurally examined brains, not by referring to an individual brain. This comparison evidently has to be probabilistic in nature due to the different subjects used for the functional and the anatomical studies.

In addition to the probabilistic anatomical labeling of functional activations, the SPM Anatomy toolbox enables the investigation of the functional response within an anatomically defined area. This type of analysis opens a new perspective on functional imaging data, since the relative change in the BOLD signal (in fMRI) or in the rCBF (in PET) is hereby calculated for a group of voxels defined by their anatomical location, not by their activation in a given contrast. Thus, functional data are assessed based on a-priori anatomical knowledge.

The potential of the combination of functional imaging data and observer-independent cytoarchitectonic mapping has been repeatedly demonstrated: Naito et al. (1999) combined anatomical data of cytoarchitectonic maps of areas 4a and 4p with the PET response to tendon vibration evoking a kinesthetic illusion to demonstrate that this motor illusion specifically activates the anterior primary motor cortex (area 4a) similar to executed motor tasks. Bodegard and coworkers combined results from PET studies examining different somatosensory tasks like shape exploration or pressure discrimination with probabilistic cytoarchitectonic maps of the human somatosensory system to show the selective involvement of its different subdivisions in different tasks (Bodegard et al., 2000a,b, 2001, 2003). Binkofski et al. (2002) demonstrated that neural activity in subarea 4p within the primary motor cortex is modulated by attention to action, while neural activity in subarea 4a is not. In a recent fMRI study, Amunts et al. (2004) showed the differential activation of left Broca's region in overlearned vs. semantic verbal fluency. Although both areas participate in verbal fluency, they do so in different ways. Left area 45 seems to be more involved in semantic aspects of language processing than area 44, while the latter is probably involved in high-level aspects of programming speech production per se.

Up to now, however, the probabilistic cytoarchitectonic maps were not integrated into a standard software package. Thus, there was no straightforward, standardized method to describe the anatomical location of the significant clusters revealed by the statistical analysis. Rather, time-consuming, customized solutions had to be set up for all studies mentioned above. Consequently, the number of studies combining structural and functional data has been very limited up to now in spite of the great benefit that can be gained from such integrated analyses.

In conclusion, the platform-independent SPM Anatomy toolbox provides a complete software package, which handles all steps for the combination of functional and anatomical data. All functions of the toolbox as described above can be accessed and configured via the same convenient graphical user interface known from the SPM software. Since the SPM Anatomy toolbox is completely integrated into the SPM architecture, it is possible to define and evaluate new functional contrasts, without having to quit and restart the toolbox. Thus, the statistical results for different tasks, comparisons or thresholds etc. can be anatomically labeled time efficiently. The combination of the probabilistic cytoarchitectonic maps and the widely used software package SPM2 via an easy-to-use graphical user interface represents a major advantage over previous "hand-made" solutions for probabilistic anatomical labeling. This development should now enable the routine use of as anatomical references for functional activations.

The published probabilistic maps (Table 1) are available at www.fz-juelich.de/ime/ime_brain_mapping in both Analyze or MINC format or via the mirror site at www.bic.mni.mcgill.ca/cytoarchitectonic. The SPM Anatomy toolbox will be released as part of the SPM2 toolbox collection. The software (including the probabilistic maps and pre-calculated MPMs) will then be available for download at www.fz-juelich.de/ime/ime_brain_mapping.

Acknowledgments

This Human Brain Project/Neuroinformatics research was funded by the National Institute of Biomedical Imaging and Bioengineering, the National Institute of Neurological Disorders and Stroke and the National Institute of Mental Health. K.Z. and G.R.F. acknowledge additional funding by the Deutsche Forschungsgemeinschaft (KFO-112). K.A. was supported by the Deutsche Forschungsgemeinschaft (Schn 362/13-2).

References

Amunts, K., Zilles, K., 2001. Advances in cytoarchitectonic mapping of the human cerebral cortex. Neuroimaging Clin. N. Am. 11 (2), 151–169.

Amunts, K., Schleicher, A., Burgel, U., Mohlberg, H., Uylings, H.B., Zilles, K., 1999. Broca's region revisited: cytoarchitecture and intersubject variability. J. Comp. Neurol. 412, 319–341.

Amunts, K., Malikovic, A., Mohlberg, H., Schormann, T., Zilles, K., 2000. Brodmann's areas 17 and 18 brought into stereotaxic space—where and how variable? NeuroImage 11, 66–84.

Amunts, K., Weiss, P.H., Mohlberg, H., Pieperhoff, P., Eickhoff, S., Gurd, J.M., Marshall, J.C., Shah, N.J., Fink, G.R., Zilles, K., 2004. Analysis of verbal fluency in cytoarchitectonically defined stereotaxic spacethe roles of Brodmann's areas 44 and 45. NeuroImage 22, 42–56.

Binkofski, F., Fink, G.R., Geyer, S., Buccino, G., Gruber, O., Shah, N.J., Taylor, J.G., Seitz, R.J., Zilles, K., Freund, H.J., 2002. Neural activity in human primary motor cortex areas 4a and 4p is modulated differentially by attention to action. J. Neurophysiol. 88, 514–519.

Bodegard, A., Geyer, S., Naito, E., Zilles, K., Roland, P.E., 2000a. Somatosensory areas in man activated by moving stimuli: cytoarchitectonic mapping and PET. NeuroReport 11, 187–191.

Bodegard, A., Ledberg, A., Geyer, S., Naito, E., Zilles, K., Roland, P.E., 2000b. Object shape differences reflected by somatosensory cortical activation. J. Neurosci. 20, RC51.

Bodegard, A., Geyer, S., Grefkes, C., Zilles, K., Roland, P.E., 2001. Hierarchical processing of tactile shape in the human brain. Neuron 31, 317–328.

Bodegard, A., Geyer, S., Herath, P., Grefkes, C., Zilles, K., Roland, P.E., 2003. Somatosensory areas engaged during discrimination of steady pressure, spring strength, and kinesthesia. Hum. Brain Mapp. 20, 103–115.

Brett, M., Johnsrude, I.S., Owen, A.M., 2002. The problem of functional localization in the human brain. Nat. Rev., Neurosci. 3, 243–249.

Brodmann, K., 1909. Vergleichende Lokalisationslehre der Großhirnrinde. Barth, Leipzig.

Collins, D.L., Neelin, P., Peters, T.M., Evans, A.C., 1994. Automatic 3D intersubject registration of MR volumetric data in standardized Talairach space. J. Comput. Assist. Tomogr. 18, 192–205.

Crespo-Facorro, B., Kim, J.J., Andreasen, N.C., O'Leary, D.S., Wiser, A.K., Bailey, J.M., Harris, G., Magnotta, V.A., 1999. Human frontal cortex: an MRI-based parcellation method. NeuroImage 10 (5), 500–519 (Nov).

Evans, A.C., Marrett, S., Neelin, P., Collins, L., Worsley, K., Dai, W., Milot, S., Meyer, E., Bub, D., 1992. Anatomical mapping of functional activation in stereotactic coordinate space. NeuroImage 1, 43–53.

Felleman, D.J., Van Essen, D.C., 1991. Distributed hierarchical processing in the primate cerebral cortex. Cereb. Cortex 1 (1), 1–47 (Jan–Feb).

Geyer, S., 2003. The Microstructural Border between the Motor and the Cognitive Domain in the Human Cerebral Cortex. Springer, Wien.

Geyer, S., Ledberg, A., Schleicher, A., Kinomura, S., Schormann, T., Burgel, U., Klingberg, T., Larsson, J., Zilles, K., Roland, P.E., 1996. Two different areas within the primary motor cortex of man. Nature 382, 805–807.

Geyer, S., Schleicher, A., Zilles, K., 1999. Areas 3a, 3b, and 1 of human primary somatosensory cortex: 1. Microstructural organization and interindividual variability. NeuroImage 10, 63–83.

Geyer, S., Matelli, M., Luppino, G., Zilles, K., 2000a. Functional neuroanatomy of the primate isocortical motor system. Anat. Embryol. (Berl) 202, 443–474.

Geyer, S., Schormann, T., Mohlberg, H., Zilles, K., 2000b. Areas 3a, 3b, and 1 of human primary somatosensory cortex. Part 2. Spatial normalization to standard anatomical space. NeuroImage 11, 684–696.

Grefkes, C., Geyer, S., Schormann, T., Roland, P., Zilles, K., 2001. Human somatosensory area 2: observer-independent cytoarchitectonic mapping, interindividual variability, and population map. NeuroImage 14, 617–631.

Grefkes, C., Weiss, P.H., Zilles, K., Fink, G.R., 2002. Crossmodal processing of object features in human anterior intraparietal cortex: an fMRI study implies equivalencies between humans and monkeys. Neuron 35, 173–184.

Holmes, C.J., Hoge, R., Collins, L., Woods, R., Toga, A.W., Evans, A.C., 1998. Enhancement of MR images using registration for signal averaging. J. Comput. Assist. Tomogr. 22, 324–333.

Kim, J.J., Crespo-Facorro, B., Andreasen, N.C., O'Leary, D.S., Zhang, B., Harris, G., Magnotta, V.A., 2000. An MRI-based parcellation method for the temporal lobe. NeuroImage 11 (4), 271–288 (Apr).

Lancaster, J.L., Rainey, L.H., Summerlin, J.L., Freitas, C.S., Fox, P.T., Evans, A.C., Toga, A.W., Mazziotta, J., 1997. Automated labeling of the human brain: a preliminary report on the development and evaluation of a forward-transform method. Hum. Brain Mapp. 5, 238–242.

Lancaster, J.L., Woldorff, M.G., Parsons, L.M., Liotti, M., Freitas, C.S., Rainey, L., Kochunov, P.V., Nickerson, D., Mikiten, S.A., Fox, P.T., 2000. Automated Talairach atlas labels for functional brain mapping. Hum. Brain Mapp. 10, 120–131.

Luppino, G., Matelli, M., Camarda, R.M., Gallese, V., Rizzolatti, G., 1991. Multiple representations of body movements in mesial area 6 and the adjacent cingulate cortex: an intracortical microstimulation study in the macaque monkey. J. Comp Neurol. 311, 463–482.

Maldjian, J.A., Laurienti, P.J., Kraft, R.A., Burdette, J.H., 2003. An automated method for neuroanatomic and cytoarchitectonic atlas-based interrogation of fMRI data sets. NeuroImage 19, 1233–1239.

Manjaly, Z., Marshall, J.C., Stephan, K.E., Gurd, J., Zilles, K., Fink, G.R., 2003. In search of the hidden: an fMRI study with implications for the study of patients with autism and with acquired brain injury. NeuroImage 19, 674–683.

Matelli, M., Luppino, G., Rizzolatti, G., 1991. Architecture of superior and mesial area 6 and the adjacent cingulate cortex in the macaque monkey. J. Comp. Neurol. 311, 445–462.

Mohlberg, H., Lerch, J., Amunts, K., Evans, A.C., Zilles, K., 2003. Probabilistic cytoarchitectonic maps transformed into MNI space. Presented at the 9th International Conference on Functional Mapping of the Human Brain, June 19–22 2003, New York, NeuroImage vol. 19(2). Academic Press, San Diego (available on CD ROM).

Morosan, P., Rademacher, J., Schleicher, A., Amunts, K., Schormann, T., Zilles, K., 2001. Human primary auditory cortex: cytoarchitectonic subdivisions and mapping into a spatial reference system. NeuroImage 13, 684–701.

Naito, E., Ehrsson, H.H., Geyer, S., Zilles, K., Roland, P.E., 1999. Illusory arm movements activate cortical motor areas: a positron emission tomography study. J. Neurosci. 19, 6134–6144.

Passingham, R.E., Stephan, K.E., Kotter, R., 2002. The anatomical basis of functional localization in the cortex. Nat. Rev., Neurosci. 3 (8), 606–616 (Aug).

Rademacher, J., Morosan, P., Schormann, T., Schleicher, A., Werner, C., Freund, H.J., Zilles, K., 2001. Probabilistic mapping and volume measurement of human primary auditory cortex. NeuroImage 13, 669–683.

Roland, P.E., Zilles, K., 1994. Brain atlases—a new research tool. Trends Neurosci. 17, 458–467.

Schleicher, A., Amunts, K., Geyer, S., Kowalski, T., Zilles, K., 1998. An

observer-independent cytoarchitectonic mapping of the human cortex using a stereological approach. Acta Stereol. 17, 75–82.

Talairach, J., Tournoux, P., 1988. Co-Planar Stereotaxic Atlas of the Human Brain. Thieme, Stuttgart.

Tzourio-Mazoyer, N., Landeau, B., Papathanassiou, D., Crivello, F., Etard, O., Delcroix, N., Mazoyer, B., Joliot, M., 2002. Automated anatomical labeling of activations in SPM using a macroscopic anatomical parcellation of the MNI MRI single-subject brain. NeuroImage 15, 273–289.

von Economo, K., Koskinas, G., 1925. Die Cytoarchitektonik der Hirnrinde des erwachsenen Menschen. Springer, Wien.

Young, J.P., Herath, P., Eickhoff, S., Choi, J., Grefkes, C., Zilles, K., Roland, P.E., 2004. Somatotopy and attentional modulation of the human parietal and opercular regions. J. Neurosci. 24, 5391–5399.

Zilles, K., Schleicher, A., Palomero-Gallagher, N., Amunts, K., 2002. Quantitative analysis of cyto- and receptor architecture of the human brain. In: Mazziotta, J., Toga, A. (Eds.), Brain Mapping, the Methods. Elsevier, pp. 573–602.